

# Nephrons require Rho-kinase for proximal-distal polarity development



SCIENTIFIC REPORTS

OPEN

SUBJECT AREAS:
EMBRYONIC INDUCTION
EPITHELIAL-MESENCHYMAL TRANSITION
APICOBASAL POLARITY
MYOSIN

Received
3 January 2013

Accepted
29 August 2013

Published
18 September 2013

Correspondence and requests for materials should be addressed to N.O.L. (nils.lindstrom@ed.ac.uk) or J.A.D. (jamie.davies@ed.ac.uk)

# Nephrons require Rho-kinase for proximal-distal polarity development

Nils O. Lindström[1,2,3], Peter Hohenstein[2,3] & Jamie A. Davies[1]

[1]Centre for Integrative Physiology, The University of Edinburgh, Hugh Robson Building, EH8 9XB, United Kingdom, [2]MRC Human Genetics Unit, Institute of Genetics and Molecular Medicine, The University of Edinburgh, Edinburgh, EH4 2XU, United Kingdom, [3]The Roslin Institute, The University of Edinburgh, Easter Bush, EH25 9RG, United Kingdom.

**Epithelial tubules must have the right length and pattern for proper function. In the nephron, planar cell polarity controls elongation along the proximal-distal axis. As the tubule lengthens, specialized segments (proximal, distal etc.) begin to differentiate along it. Other epithelia need Rho-kinase for planar cell polarity but it is not known whether Rho-kinase is involved in this way in the nephron. We show that Rho-kinase is essential for the morphogenesis of nephrons, specifically for correct cell orientation and volume. We use fluorescent reporter-models and progenitor-specific markers to demonstrate that inhibition of Rho-kinase prevents proper proximal-distal axis formation, causes segments to develop abnormally, and progenitor-cell segregation to fail. Our data demonstrate the importance of Rho-kinase in normal nephron tubulogenesis and patterning.**

Cellular polarity is a characteristic of all epithelia and the acquisition of polarity is essential for tubulogenesis during embryonic development. Understanding how cell polarities develop and are orientated *in vivo* is a major research problem: in addition, the possible importance of polarities in maintaining epithelial characteristics is also a much debated matter because renal fibrosis secondary to epithelial-mesenchymal transition is a key feature of chronic kidney failure[1,2]. Nephrons form by mesenchymal-to-epithelial transitions of progenitor cells[3]. As they differentiate, these cells acquire both an apical-basal axis across the epithelial plane and a planar proximal-distal axis along the tubule[3]. Elongation of nephron tubules is regulated by a myosin-dependent mechanism of convergent extension[4–6]. This is in turn controlled by *Wnt9b* which establishes the planar cell polarity (PCP) along the proximal-distal axis[4–6]. Central to convergent extension in other systems is the Rho-pathway[7]: in particular Rho-kinase (ROCK) regulates a range of necessary cytoskeletal processes, including microtubule stability, adherens junction formation and myosin stress-fibre formation[8–11]. Cell-culture models suggest that the Rho-signalling pathway is vital for the establishment of epithelial polarity[12–17] and *Wnt9b* deficient mice[5,6] produce ureteric bud defects similar to those caused by the inhibition of ROCK in kidney organ cultures[18]. Although, *Wnt9b* and a myosin-dependent convergent extension control aspects of nephron morphogenesis (e.g. elongation)[4], it is not clear whether ROCK is also involved. ROCK has not been studied in the context of nephron PCP, and although ROCK1 and ROCK2 knockouts are without renal phenotypes[19,20], the double knockouts, which would eliminate known redundancy, have not been made[21].

## Results

**Rho-Kinase is required for normal nephron formation.** We blocked ROCK function during nephron formation by applying ROCK-inhibitors glycyl-H1152 (hereafter H1152)[22,23] and Y27632[24], separately, to various embryonic kidney culture systems[18,25,26]. To monitor effects on nephron development we used kidneys from E12.5 *Wt1*$^{+/GFP}$ knock-in reporter mice[27] and wild-type embryos to track the early nephron and podocyte progenitors[28], and antibodies against tubule basement membrane (β-laminin) and the ureteric bud (Calbindin-D28K)[29]. ROCK-inhibited kidneys contained morphologically abnormal nephrons (Fig. 1b and Fig. S1b–d) compared to controls (Fig. 1a and Fig. S1a,c). We counted the number of morphologically normal and abnormal nephrons in treated and untreated wild-type kidneys (Fig. 1c; see Materials and Methods for scoring criteria). 61% of nephrons forming in ROCK inhibiting conditions ($n = 76$; from 3 kidneys) displayed morphological abnormalities whilst only 5% of control nephrons ($n = 58$; from 3 kidneys) did so ($p = 0.00145$ by Student's t-test).

We and others have previously shown that the ureteric bud is itself affected by ROCK inhibitors[18,25] (Fig. 1b and Fig. S1b). We tested whether the there was also a reduction in the number of nephrons, which

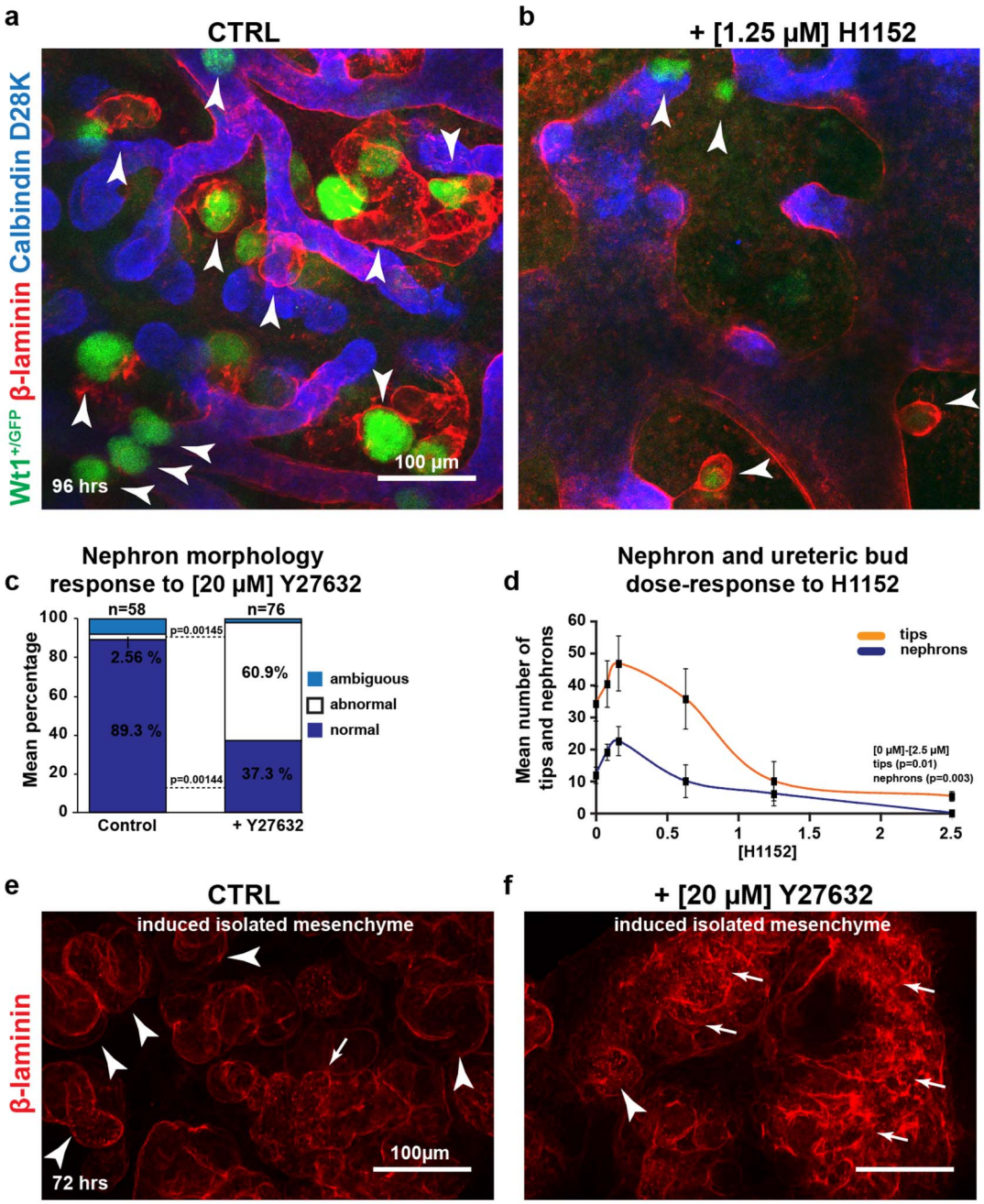


**Figure 1 | Inhibition of ROCK reduces nephron formation and disturbs normal morphology.** (a) Control culture of *Wt1*$^{+/GFP}$ kidney. (b) Culture of *Wt1*$^{+/GFP}$ kidney grown in ROCK inhibiting conditions. Nephrons indicated with arrowheads. (c) Mean percentage of abnormal, normal, and ambiguous nephrons in controls and experimental wild-type kidneys after 120 hrs of culture. P-values related to differences in categories. (d) Mean number of ureteric bud tips and nephrons plotted against specified concentrations after 96 hrs of culture. Error bars indicates SEM in both graphs. P-values related to reduction in tip-numbers. (e) Induced isolated mesenchyme in control conditions and (f) ROCK conditions. Abnormal epithelialisation (arrows), normal nephrons (arrowheads). Antibody stains and culture times as specified on images.

there was (Student's t-test p = 0.003 for control vs. 2.5 μM H1152), and whether this correlated with a decrease in the number of ureteric bud tips (Fig. 1d) (n = 25 kidneys), which it did (r = 0.94, Pearson coefficient, using all samples from control and all inhibitor concentrations; Student's t-test p = 0.01 for control vs. 2.5 μM H1152). These data raised the possibility that the effects of ROCK inhibition on nephron morphogenesis were secondary to its effects on ureteric bud, We therefore removed the ureteric bud from the system by combining metanephric mesenchyme with spinal cord, a known inducer of nephrogenesis[30,31]. In controls, nephrons developed normally (Fig. 1e and Fig. S1f) but inhibition of ROCK still caused the formation of aberrant and tangled epithelial structures (Fig. 1f and Fig. S1f). As suggested by previous studies, the nephron mesenchymal-to-epithelial transition itself is not blocked by ROCK inhibition[18,25]. To test whether the timing of ROCK inhibition influenced the degree to which nephron formation was disturbed, we added the inhibitor at different time-points or withdrew it once added (Fig. S2); E12.5 kidneys were used. Withdrawing the inhibitor after 24 hrs or 48 hrs and culturing in normal medium to a total of 72 hrs allowed nephrogenesis to recover to produce 90% and 60%, respectively, of the total nephrons found in controls. Cultures continuously maintained

in inhibitor-conditions (72 hrs) developed only 10% of the total nephrons found in controls. The recovery of nephron numbers seen when the inhibitor was removed after 24 hrs or 48 hrs of culture was significant compared to samples continuously treated with inhibitor ($p = 0.0001$, $p = 0.0003$). Adding the inhibitor only at a later time point between 48 hrs and 72 hrs also led to fewer nephrons forming compared to controls (49% of control, $p = 0.007$): this was not significantly different from those samples exposed to a 24 hr dose of inhibitor at the start of the experiments ($p = 0.14$). Morphological defects were also seen in nephrons that formed in induced isolated mesenchyme when ROCK was inhibited only after epithelialisation had taken place, during the period of nephron segmentation (Fig. S1g). Together, these data indicate that the effect of ROCK inhibition of nephrons is direct and not secondary to the effect on ureteric bud. qRT-PCR analysis of markers for the major kidney components and processes (*Six2* - nephron progenitors, *GDNF* - ureteric branching, *Wnt4* and *Lhx1* - nephron induction, *Hoxb7* and *Wnt11* – ureteric bud) indicated that ROCK inhibition had no significant effect on their expression (Fig. S1e). Hereafter only H1152 was used for experimental consistency and because kinase-inhibition studies have demonstrated a greater degree of specificity for Rho-kinase by H1152 compared to Y-27632[23].

**Rho-Kinase is required for tubule morphogenesis.** Nephron development is highly dynamic so, to visualise and characterise the nephron defects, we set up time-lapse cultures of kidney from *Pax8$^{Cre}$;YFP$^{lox\text{-}stop}$* reporter mice[32,33]. *Pax8* is expressed in the ureteric bud, in induced nephron progenitor cells, and in the nephron itself[34]. *Pax8$^{Cre}$;YFP$^{lox\text{-}stop}$* kidneys stably express *YFP* in all nephron lineages (Movie 1: the *Pax8$^{Cre}$;YFP$^{lox\text{-}stop}$* reporter mouse cross and lineage tracing experiments are to be fully described in Berry *et al.* in preparation). We added the ROCK inhibitor either at the start of the experiment, before nephrons formed (Fig. 2b), or only after 48 hrs of culture (Fig. S3a and Movie 2) when nephrons had epithelialised and started segmentation. Both cases resulted in a variety of defects. Nephrons that formed in ROCK-inhibitor conditions epithelialised (i.e. they expressed *Cdh1*) and initiated segmentation (i.e. they expressed *Jag1*-in their medial domain) (Fig. 2b and Fig. S3a) in a similar manner to controls (Fig. 2a). Consistently, however, they failed to elongate normally and instead rounded up into cyst-like structures (Movie 2).

Kidney tubules elongate along their proximal-distal axis by a mechanism of convergent extension, resulting in cells that have completed the process being positioned at an angle perpendicular to that of the direction of the tubule[4]. We investigated whether the morphological defects could be caused by the cells being abnormally polarised. To do this we generated cell 3D reconstructions and measured the orientation of these nephron cells within the tubules, as described elsewhere[4] and in Materials and Methods. We measured each cell's orientation compared to the direction of the tubule and calculated the deviation of this value from the 90° angle expected by a perfectly perpendicularly aligned cell. The cell angles were measured as positive numbers, regardless of the direction of the deviation, in order to gain an absolute measure of error that would not be cancelled by equal errors in opposite directions by different cells. In controls, the mean deviation was 17° (Fig. 2c, f; $n = 83$ cells from 7 nephrons). ROCK inhibitor treated nephrons displayed two distinct sets of cell populations, those which were located within morphologically more normal epithelial tubules (Fig. 2d, g; $n = 85$ cells; from 6 nephrons) and those within bloated portions of tubules (Fig. 2e, h; $n = 61$ cells from 5 nephrons). The cells in the more normal tubules averaged a higher mean deviation 25° compared to controls (Fig. 2g; 25°, $p = 0.006$). Those cells located within bloated tubules displayed a much greater degree of deviation 33° compared to controls ($p = 4 \times 10^{-6}$).

In other tissues, ROCK activity is important for the regulation of cell size[35,36]. We tested whether the cell size was also altered by ROCK inhibition by analysing the volume of the cells (measured by 3D reconstruction from optical sections). ROCK-inhibited cells from both 'normal' and bloated nephron segments showed a large increase (+78%) in cell volume compared to controls ($p = 6 \times 10^{-10}$, $n = 94$ cells from control conditions vs. 159 cells from H1152 conditions) (Fig. S3b).

**Rho-Kinase is required for progenitor segregation but not differentiation.** The proximal-distal axis is populated by domains containing different progenitor cells that will give rise to segment-specific lineages. To test whether the cell-polarisation defects affected the specification or location of these progenitor cell populations we performed antibody stains against segment-specific proteins and examined kidneys for regions of abnormal expression overlap. *Wt1* and *Podxl* were used to detect glomerular/podocyte progenitors. *Lotus tetragonolobus* lectin (LTL) for proximal tubule cells and *Jag1* for Loop of Henle and proximal tubule progenitors[28,37–40]. The distal tubule displays strong Cdh1 and is negative for the other markers used[38]. Remarkably, in controls only 4/891 (0.4%) of nephrons examined displayed spatial overlap of segment markers in any area of the nephron (Fig. S4a). In ROCK-inhibitor treated samples, this overlap was still uncommon but increased 10-fold (25/549, 4.5%; Fig. S4a). A Chi Square test was significant to $p = 0.001$, d.f. $= 1$ $x^2 = 29.0$. Overlap between WT1$^+$ and JAG1$^+$ domains (i.e. glomerular podocyte and proximal/medial tubule) accounted for 80% of these cases. *Wt1* and *Jag1* are expressed during the earliest stages of nephron development, whilst LTL binding and *Podxl* expression is initiated at later time-points. We carried out confocal scans at higher magnification (60×) and these showed a range of segmentation abnormalities: engulfed glomeruli (Fig. 3a and Fig. S4b), overlap of segment-specific expression (Fig. 3b and Fig. S4c), and what appeared as loosely structured glomeruli (Fig. 3c and Fig. S4d).

As ROCK activity can also affect differentiation[41] we used qRT-PCR to analyse the expression of 11 genes exclusively expressed in specific nephron-segments (Fig. 3d). It would be expected from data presented above that by applying the ROCK inhibitor we would reduced nephron numbers by ~ 70% (Fig. 1d), thus, any important reduction would have to be greater than this. Expression levels were significantly decreased for 6/11 genes analysed; however, they were decreased by an average of 64% (Fig. 3d), not far from the expected 70% decrease. This suggests that the reduction in gene expression is caused by the decrease in nephron formation rather than by loss of differentiation of any particular nephron segment.

We focused on the nephron defects that displayed abnormal segregation of segment-progenitor cells (Fig. 3b). To determine whether the WT1$^+$ podocyte progenitor cells (Fig. 3b) also extended into the tubular portion of nephrons we again used the *Pax8$^{Cre}$;YFP$^{lox\text{-}stop}$* reporter to mark all nephron cells (Fig. 4a). Nephrons displayed WT1$^+$ cells within tubular regions that were also CDH1$^+$ (Fig. 4a). We confirmed this by 3D visualisation (Fig. 4b, Fig. S5a). Another defect perhaps related to tubule identities was the occurrence of nephrons with two connections to the ureteric bud. These were fused at their JAG1$^+$ proximal domain (Fig. 4c and Fig. S5c). To confirm that such nephrons were indeed caused by nephrons abnormally fusing to other nephrons we set up time-lapse experiments of *Wt1$^{+/GFP}$* knock-in reporter mice. In ROCK-inhibitor treated *Wt1$^{+/GFP}$* kidneys, nephrons occasionally came head-to-head and fused with each other (Fig. 4d and Movie 4). In experimental conditions, 6/6 kidneys displayed such nephron-to-nephron fusions. The number of fusions per kidney ranged from 5 sets to only 1 (average was 2.7). In control conditions (Fig. 4d and Movie 3) such nephron-to-nephron fusions were less frequent ($p = 0.049$). 4/6 control kidneys displayed fusions at an average of 0.83 fusions per kidney.

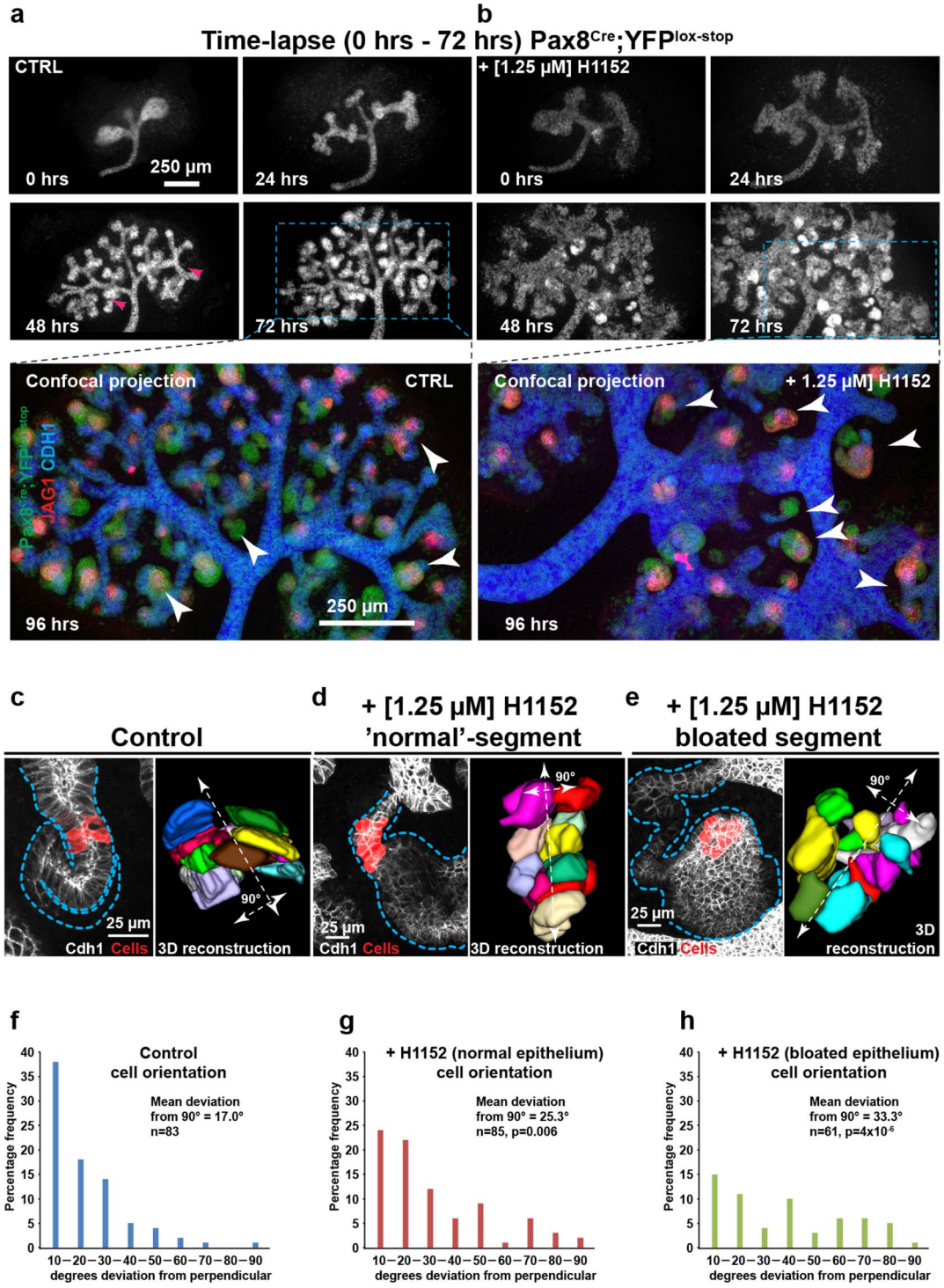


**Figure 2 | Inhibition of ROCK perturb normal planar cell polarity and elongation.** Time-lapse of *Pax8$^{Cre}$YFP$^{lox\text{-}stop}$* kidneys in (a) control conditions, or in (b) ROCK inhibitor conditions. Boxed area - confocal scans performed on same kidneys. Nephrons indicated with arrowheads. 3D reconstructions of tubular cells in (c) control conditions (d, e) ROCK inhibiting conditions. Total cell numbers shown on cell-orientation graphs. Graphs display the percentage frequency of cells exhibiting a particular angle of deviation from the perpendicular. Antibody stains and culture times as specified on images. p-values were calculated using Student's t-tests.

## Discussion

As the nephron forms, it develops multiple segments that express genes and display properties distinct to each segment. During the process of segmentation it also undergoes a series of complex morphogenetic changes; for instance it connects with the ureteric bud, it elongates, and it develops the Bowman's capsule. This division of the nephron into domains is evident from the stage directly after epithelialisation[37,42,43]. Because the segmentation, patterning, elongation, and morphogenesis occur simultaneously, they are likely to at some level be co-dependent. Here, we have demonstrated that Rho-kinase (ROCK) activity is required for both morphogenesis and the patterning of the nephron. With reduced ROCK activity, serious failures of morphogenesis occur and we show that these are associated with the disorientation of cell axes within the nephron tubule.

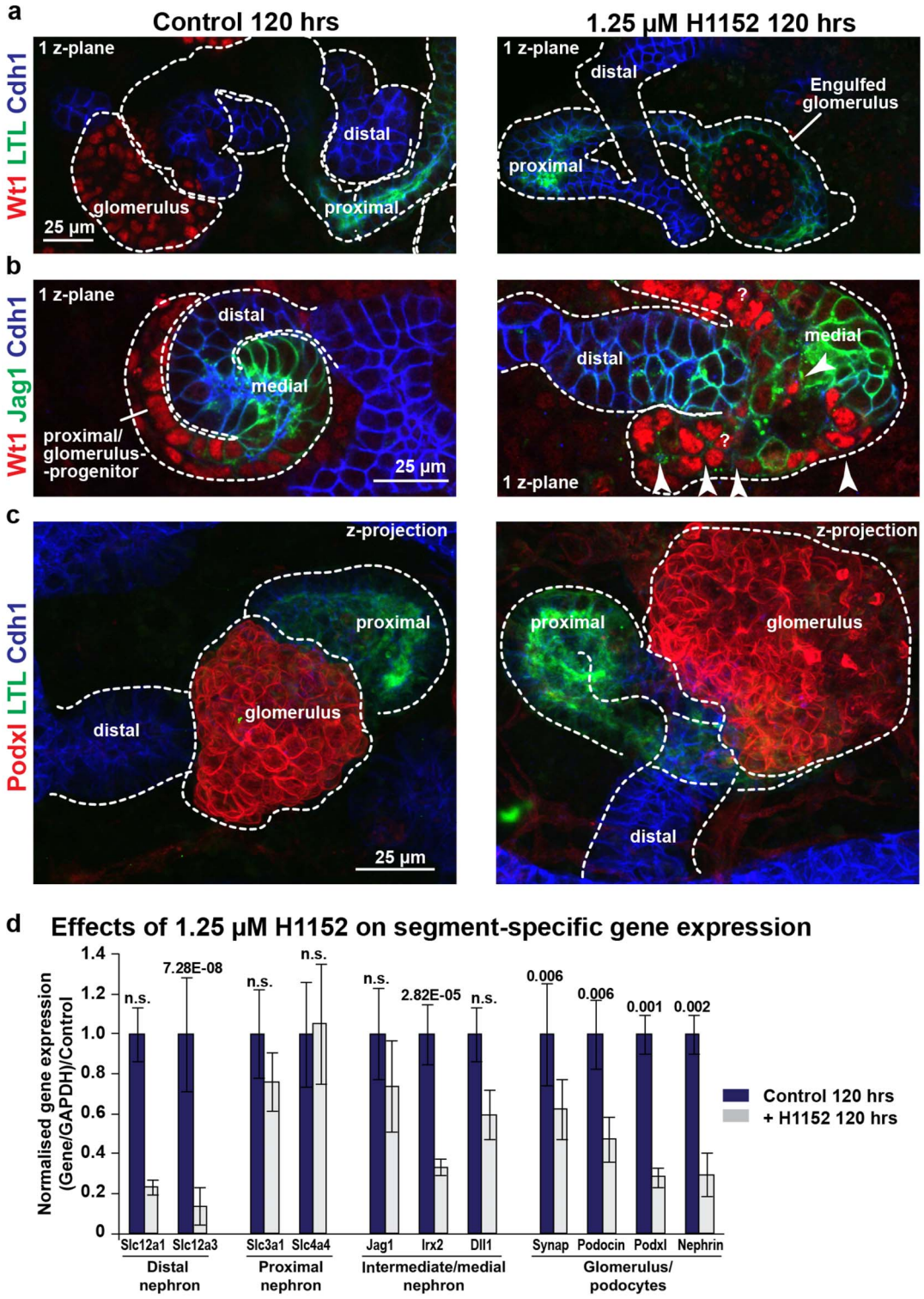


**Figure 3 | ROCK is required for tubule morphogenesis.** Nephrons in ROCK inhibitor conditions display a range of defects as characterised using segment-specific markers. (a) $WT1^+$ glomeruli forming within $LTL^+$ proximal tubule. (b) $WT1^+$ and $JAG1^+$ cells overlap in their expression domains. (c) $PODXL^+$ podocytes within glomeruli are poorly packed and fragment from glomeruli. Dashed lines outline nephrons. Arrowheads indicate cells with overlapping expression of WT1 and JAG1. (d) qRT-PCR analysis on segment-specific genes. RNA was extracted from whole treated kidneys and the qRT-PCR analysis was performed against genes expressed in specific cell-types within particular nephron segments. Error bars indicate SEM, p = values stated in Methods section. Antibody stains as specified on images.

In Xenopus nephrons, the elongation of the nephron tubules is regulated via a process of convergent extension[4]. This elongation is dependent on Wnt-signalling and a mechanism which controls the precise alignment of cell axes[4]. Mouse nephrons rely on a similar alignment of cells as the nephron elongates, and this requires Wnt9b-PCP signalling[6] which is associated with JNK activation and therefore probably with the PCP pathway. Because ROCK is known to be activated in the PCP pathway[44] our work therefore brings these

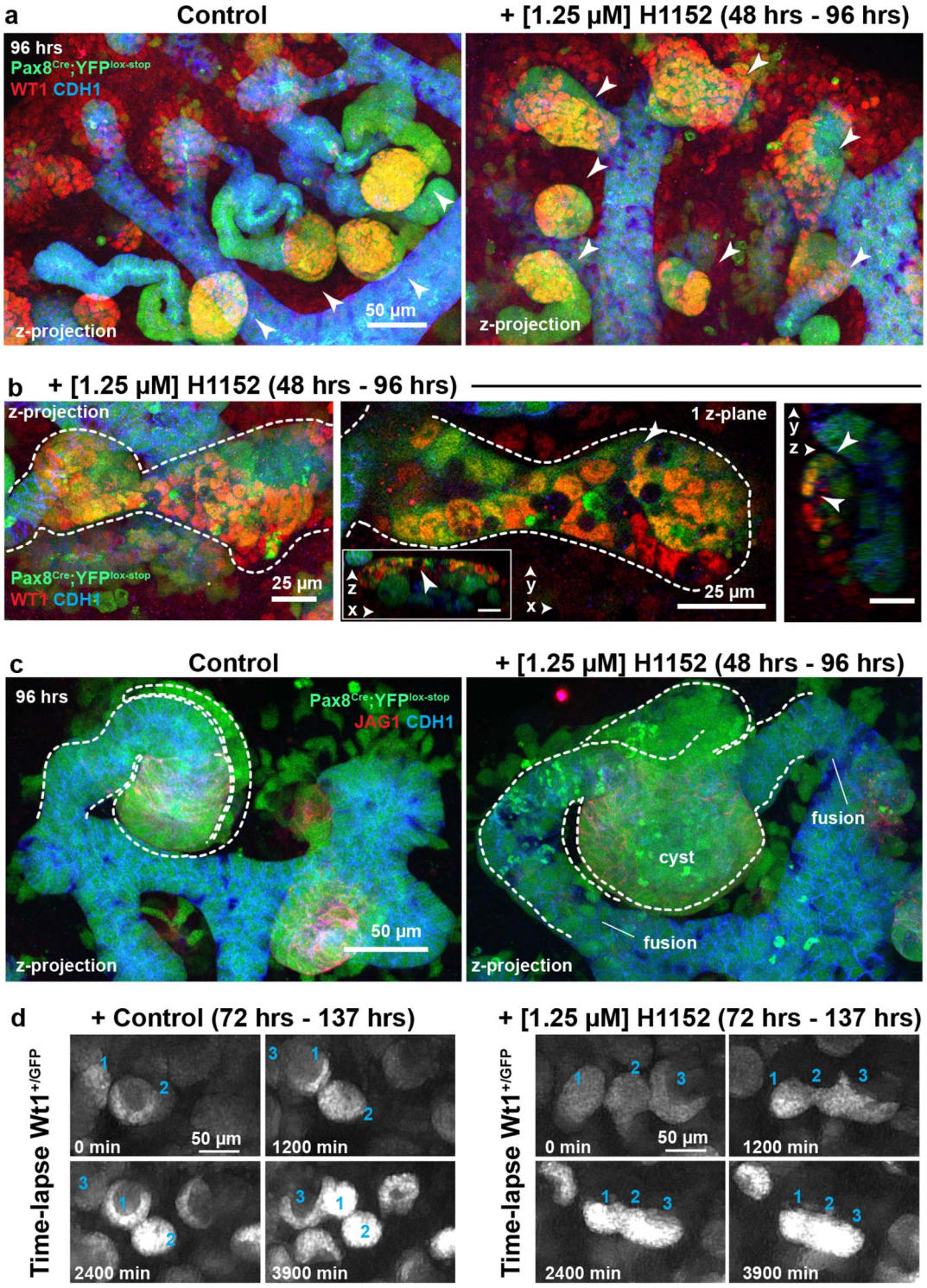


**Figure 4 | ROCK is necessary for progenitor cell segregation and segment identity.** Confocal projections of *Pax8*$^{Cre}$*YFP*$^{lox\text{-}stop}$ kidneys cultured in control or in ROCK inhibiting conditions (a). Arrowheads indicate nephrons. (b) High magnification of WT1$^{+}$ tubular region. Arrowheads indicate WT1$^{+}$ and CDH1$^{+}$ cells. (c) Nephrons in control conditions and in ROCK inhibiting conditions, the latter fused to another nephron. (d) Time-lapse of *Wt1*$^{+/GFP}$ kidney in control and ROCK inhibiting conditions, the latter displaying fusion of three GFP$^{+}$ glomeruli. Antibody stains and culture times as specified on images.

observations together to suggest that the PCP pathway acts through ROCK to control cell orientation in the nephron tubule.

ROCK is also required for normal cell migration of pre-epithelial nephron cells[25]. Although, it is not known at what precise stage the nephron is patterned into separate segments, it is known that, the renal vesicle already displays polarised gene expression directly after epithelialisation[37]. One possibility is that the specification of nephron segment identities begins prior to epithelialisation when mesenchymal nephron progenitor-cells aggregate and prepare for a mesenchymal-to-epithelial transition. If so, this could indicate that some of the defects observed here result from abnormal migration of cells during pre-epithelial stages of nephron development. This is

however unlikely to be the sole mechanism as post-epithelial nephrons are also affected by inhibition of ROCK but it raises questions regarding the importance of cell-migration for early nephron patterning.

Other consequences of losing normal ROCK activity included the failure of some nephrons to connect with the ureteric bud (Figure 2b), the abnormal positioning of the glomerulus within the tubule (Figure 3a), and the disorderly segregation of different nephron segments along the tubules (Figure 3b). ROCK serves an important function for the remodelling of epithelia in other tissues via myosin-dependent mechanisms[26,45] and in Drosophila, actin-myosin tension is known to be required for the maintenance of compartment boundaries[46]. Since ROCK is an activator of myosin, it is possible that in kidneys too, proper epithelial remodelling and compartment boundary formation require adequate actin-myosin tension, and this is required for segment segregation. Our data highlight the importance of integrating the mechanisms driving the morphogenesis of the nephron with those that regulate the differentiation programmes that are occurring as the nephron segments.

## Methods

**Animal experiments.** All animal experiments were approved by the Edinburgh University Animal Welfare and Ethical Review Body (AWERB). All animals were kept at the MRC Human Genetics Unit and University of Edinburgh animal facilities. All mice were kept according to regulations specified by the Home Office. Animals were kept and bred under P.H. Project Licence 60/3788 as approved by the Home Office.

**Organ cultures.** Kidneys were isolated from E11.5–E12.5 mice. *Wt1*$^{+/GFP}$ (Wt1$^{tm1Nhsn}$)[27] mice were crossed with CD1. *Pax8*$^{+/Cre}$ (Pax8$^{tm1(cre)Mbu}$) mice[33] were crossed to *Rosa26*$^{eYFP/eYFP}$ (Gt(ROSA)26$^{Sortm1(EYFP)Cos}$) animals[32]; a total of 35 *Pax8*$^{Cre}$;*YFP*$^{lox\text{-}stop}$ reporter kidneys were used. 14 in control conditions, 9 with H1152 added at 0 hrs, 7 with H1152 added at 48 hrs, and 5 with H1152 added at 72 hrs. 8 kidneys were used for time-lapse. Kidneys were cultured as previously described by Michael *et al.*[18]. Isolated mesenchyme was induced using E11.5 dorsal spinal cord in transfilter cultures with the mesenchyme being placed on the top and the spinal cord at the bottom. Controls were carried out using cultures of nephrons formed in transfilter spinal cord-induce mesenchyme where the spinal cord was removed after 24 hrs of induction in order to test whether the effects of inhibitors, on nephrons, were direct (and not secondary to effects on the spinal cord). Control conditions contained an equal volume of inhibitor vehicle. Inhibitors were added at the beginning of culture (t = 0) unless otherwise specified. Culture medium was changed every three days unless otherwise specified.

**Quantification of kidney morphology and nephron formation.** To quantify the kidney response to ROCK inhibitor, E11.5 kidneys were cultured and treated with a range of ROCK inhibitor concentrations (0, 0.08, 0.16, 0.63, 1.25, and 2.5 μM) for 96 hrs and stained against ureteric bud marker Calbindin D-28K and ureteric bud and nephron marker laminin. Ureteric bud tips and nephrons were counted for each kidney (25 kidneys were used).

The inhibitor-timing experiments were performed by culturing kidneys for 72 hrs in the following conditions (i) control-72 hrs; (ii) 1.25 μM H1152 0–24 hrs + control 24–72 hrs; (iii) 1.25 μM H1152 0–48 hrs + control 48–72 hrs; (iv) 1.25 μM H1152 0–78 hrs; (v) control 0–48 hrs + 1.25 μM H1152 48–72 hrs (26 kidneys were used).

To determine whether nephron segments were forming normally, with respect to morphology and differentiation, a total of 9 kidneys were set up in control and a total of 9 in H1152 conditions and cultured for 120 hrs. In sets of 3 controls and 3 experimental samples, kidneys were stained for Wt1, Jag1, Cdh1; Wt1, LTL, Cdh1; or Podxl, LTL, Cdh1. In control and H1152 conditions 328 and 134 Wt1, LTL, Cdh1 nephrons were analysed, 366 and 300 Wt1, Jag1, Cdh1 nephrons; and 197 and 115 Podxl, LTL, Cdh1 nephrons. Nephrons were visually scored for abnormal overlap of markers as compared to controls. Thus 891 nephrons in control and 549 nephrons in H1152 conditions were analysed in total.

To quantify nephron abnormality in response to ROCK inhibition, E11.5 kidneys were cultured for 120 hrs. The ROCK inhibitor was added after 48 hrs to focus on defects caused by morphogenesis rather than formation. Cultures were stained for β-laminin and Cdh1 to show the basement membrane and the morphology of the nephrons and samples were subsequently scanned using confocal microscopy. Samples used 3 kidneys per treatment and such nephrons that were clearly identifiable were individually staged according to GUDMAP ontology (www.gudmap.org) and Little et al 2007[47]; 58 nephrons were scored for control conditions and 72 nephrons for H1152 conditions. Nephrons were subsequently categorised according to morphology - using both the β-laminin and Cdh1 antibody stains as visual markers. Nephrons with obvious morphological abnormal tubules and structures were scored as 'abnormal', and such that were typical of stage and morphology were scored 'normal'. Where nephrons could not with certainty be assigned normal or abnormal morphology scores, these were classified as ambiguous.

**3D reconstructions, volumetric analyses, cell orientation.** Confocal stacks (1 μm steps, captured at 60 ×, 1024 × 1024 pixels at 0.2071602 μm/pixel) of whole nephrons were loaded into TrakEM2 - Fiji (http://fiji.sc/). The automatic segmentation tools were found to be insufficient in separating individual cells whereas manual marking was found to be more robust and was therefore utilised. Cells were thus manually marked throughout each cell's z-plane. The annotated cells were exported as tiff-stacks and remerged with the original stacks. Cell orientations were measured against the plane of the nephron segment where the cells were located. The cell orientation was taken as the broadest point of the cell. All angles measured were within 0°–180°degrees. The angles were plotted against the frequency. The deviation from 90° (which would indicate a cell perfectly orthogonal to the plane) was used for statistical comparison between groups. The cell volumes of the reconstructed cells were automatically calculated using TrakEM2. A total of 30-kidneys were scanned at low magnification (10×), 8 control nephrons and 13 ROCK-inhibitor treated nephrons were scanned at 60×. 7, 6, and 5, control, 'normal', and 'bloated', tubules were used for the cell reconstructions.

**Immunohistochemistry and inhibitors.** Kidneys were fixed on filters in −20°C methanol prior to 1 hr washes and antibody incubations in PBS. Primary and secondary antibody incubations were carried out at 4°C over night. Antibodies were diluted in 1 × PBS. Samples were mounted in 1 : 1 Glycerol:1 × PBS or Vectashield, sealed with Lizzie/Pink varnish, and visualised on a Leica TCS-NT laser scanning confocal microscope, Zeiss Axio Imager.A1 or Nikon A1R. Time-lapse imaging was carried out using a Nikon TiE inverted microscope. Primary antibodies were used at the following concentrations: anti-Laminin (L9393/SIGMA), anti-CD15 (M0733/DAKO), anti-CDH1 (610181/BD), anti-Pan-cytokeratin (C2562/SIGMA), anti-WT1 (sc-192/SANTA CRUZ), anti-JAG1 (R&D Systems). Nuclei were stained with TO-PRO-3 iodide (T3605/MOLECULAR PROBES), 1 : 250. Secondary antibodies were purchased from SIGMA and Molecular Probes. Rho-kinase inhibitor Y27632 (Y0503/SIGMA) was reconstituted in $dH_2O$, stored at −20°C and used at 10 μM–20 μM; 20 μM was used. Glycyl-H1152 dihydrochloride (2485/TOCRIS) was reconstituted in $dH_2O$, stored at −20°C and used at a range of 1.25 μM–2.5 μM; 1.25 μM was used in all experiments except for experiment shown in (Fig. 1d) looking at dosage-response.

**Segment-specific gene expression.** To isolate RNA, cultured control and experimental kidneys were placed in RNALater (Ambion) for stabilisation. A minimum of 9 kidneys were used per condition, with 3 kidneys per replicate. The RNA isolated and used for quantification was the same in Figure 3 and Figure S1. RNA isolation was performed using RNeasy Micro kits (Qiagen) from the whole kidneys. 500 μg RNA was used for cDNA synthesis using SuperScript II Reverse Transcriptase (Invitrogen) with Random Primers (Promega). qRT-PCR assays were performed using the Universal Probe Library (Roche) and all primers/probes were designed using the Universal Probe Library Assay Design Center (http://www.roche-applied-science.com/sis/rtpcr/upl/index.jsp?id=UP030000). The primers and probes used were: *Slc12a1* (F: tatttgcacaaacggagtgg R: aagctccgggaaatcaggta probe:10) p = 0.109; *Slc12a3* (F: cctccatcaccaactcacct R: ccgcccacttgctgtagta probe:12) p = $7.28 \times 10^{-8}$; *Slc3a1* (F: ccatgtcaacggtgtaacca R: gccagctggagtttccatac probe:102) p = 0.316; Slc4a4 (F: actgtctccagtgcaagtagga R: tgtcagattcctgtgggtca probe:26) p = 0.579; *Jag1* (F: gaggcgtcctctgaaaaaca R: acccaagccactgttaagaca probe:6) p = 0.279; *Irx2* (F: gaagcaaggaggagagttcaga R: gtgagcgagtcgacgtgtag probe:98) p = $2.85 \times 10^{-5}$; *Dll1* (F: gggcttctctggcttcaac R: taagagttgccgaggtccac probe:103) p = 0.181; *Synap* (F: gtagccaggtgagccaagg R: ttttcggtgaagcttgtgc probe:67) p = 0.006; *Podocin* (F: ccatctggttctgcataaagg R: ccaggacctttggctcttc probe:38) p = 0.006; *Podxl* (F: cctgcatctcactcccataat R: tctgttgatgttgtggcactt probe:21) p = 0.001; *Nephrin* (F: aacatccagctcgtcagcat R: agggctcacgctcacaac probe:25) p = 0.002; *Hoxb7* (F: ctggatgcgaagctcagg R: ccgagtcaggtagcgattgta probe:1) p = 0.119; *Wnt11* (F: gagctcgccccccaactac R: ggcatacacgaaggctgact probe:85) p = 0.231; *Wnt4* (F: ctggactccctccctgtctt R: atgcccttgtcactgcaaa probe:62) p = 0.489; *Lhx1* (F: aatgcaacctgaccgagaag R: cgcatttggtaccgaaacat probe:7) p = 0.112; *Gdnf* (F: tccaactgggggtctacg R: gacatcccataacttcatcttagagtc probe:70) p = 0.935; *Six2* (F: caagtcagcaactggttcaaga R: actgccattgagcgagga probe:5) p = 0.275. Statistical analyses were performed using Student's t-tests against controls. Every TaqMan assay used a mouse *Gapdh* internal control (Roche) and was run twice in repeated triplicates. The assays were run on a Light Cycler 480 (ROCHE) using 384-well plates, 60 × cycles of 95°C 10 s, 60°C 30 s, 72°C 1 s.


1. Kriz, W., Kaissling, B. & Le Hir, M. Epithelial-mesenchymal transition (EMT) in kidney fibrosis: fact or fantasy? *J Clin Invest* **121**, 468–474 (2011).
2. Iwano, M. *et al.* Evidence that fibroblasts derive from epithelium during tissue fibrosis. *J Clin Invest* **110**, 341–350 (2002).
3. Saxen, L. *Organogenesis of the Kidney.* (Cambridge University Press, 1987).
4. Lienkamp, S. S. *et al.* Vertebrate kidney tubules elongate using a planar cell polarity-dependent, rosette-based mechanism of convergent extension. *Nat Genet* (2012).
5. Carroll, T. J., Park, J. S., Hayashi, S., Majumdar, A. & McMahon, A. P. Wnt9b plays a central role in the regulation of mesenchymal to epithelial transitions underlying organogenesis of the mammalian urogenital system. *Dev Cell* **9**, 283–292 (2005).
6. Karner, C. M. *et al.* Wnt9b signaling regulates planar cell polarity and kidney tubule morphogenesis. *Nat Genet* **41**, 793–799 (2009).

7. Habas, R., Kato, Y. & He, X. Wnt/Frizzled activation of Rho regulates vertebrate gastrulation and requires a novel Formin homology protein Daam1. *Cell* **107**, 843–854 (2001).
8. Sahai, E. & Marshall, C. J. ROCK and Dia have opposing effects on adherens junctions downstream of Rho. *Nat Cell Biol* **4**, 408–415 (2002).
9. Ridley, A. J. & Hall, A. The small GTP-binding protein rho regulates the assembly of focal adhesions and actin stress fibers in response to growth factors. *Cell* **70**, 389–399 (1992).
10. Nobes, C. D. & Hall, A. Rho, rac, and cdc42 GTPases regulate the assembly of multimolecular focal complexes associated with actin stress fibers, lamellipodia, and filopodia. *Cell* **81**, 53–62 (1995).
11. Amano, M. *et al.* Phosphorylation and activation of myosin by Rho-associated kinase (Rho-kinase). *J Biol Chem* **271**, 20246–20249 (1996).
12. Cohen, D., Brennwald, P. J., Rodriguez-Boulan, E. & Musch, A. Mammalian PAR-1 determines epithelial lumen polarity by organizing the microtubule cytoskeleton. *J Cell Biol* **164**, 717–727 (2004).
13. Martin-Belmonte, F. *et al.* Cell-polarity dynamics controls the mechanism of lumen formation in epithelial morphogenesis. *Curr Biol* **18**, 507–513 (2008).
14. O'Brien, L. E. *et al.* Rac1 orientates epithelial apical polarity through effects on basolateral laminin assembly. *Nat Cell Biol* **3**, 831–838 (2001).
15. Rajasekaran, S. A. *et al.* Na,K-ATPase beta-subunit is required for epithelial polarization, suppression of invasion, and cell motility. *Mol Biol Cell* **12**, 279–295 (2001).
16. Rogers, K. K., Jou, T. S., Guo, W. & Lipschutz, J. H. The Rho family of small GTPases is involved in epithelial cystogenesis and tubulogenesis. *Kidney Int* **63**, 1632–1644 (2003).
17. Yu, W. *et al.* Involvement of RhoA, ROCK I and myosin II in inverted orientation of epithelial polarity. *EMBO Rep* **9**, 923–929 (2008).
18. Michael, L., Sweeney, D. E. & Davies, J. A. A role for microfilament-based contraction in branching morphogenesis of the ureteric bud. *Kidney Int* **68**, 2010–2018 (2005).
19. Thumkeo, D. *et al.* Targeted disruption of the mouse rho-associated kinase 2 gene results in intrauterine growth retardation and fetal death. *Mol Cell Biol* **23**, 5043–5055 (2003).
20. Shimizu, Y. *et al.* ROCK-I regulates closure of the eyelids and ventral body wall by inducing assembly of actomyosin bundles. *J Cell Biol* **168**, 941–953 (2005).
21. Thumkeo, D., Shimizu, Y., Sakamoto, S., Yamada, S. & Narumiya, S. ROCK-I and ROCK-II cooperatively regulate closure of eyelid and ventral body wall in mouse embryo. *Genes Cells* **10**, 825–834 (2005).
22. Sasaki, Y., Suzuki, M. & Hidaka, H. The novel and specific Rho-kinase inhibitor (S)-(+)-2-methyl-1-[(4-methyl-5-isoquinoline)sulfonyl]-homopiperazine as a probing molecule for Rho-kinase-involved pathway. *Pharmacol Ther* **93**, 225–232 (2002).
23. Tamura, M. *et al.* Development of specific Rho-kinase inhibitors and their clinical application. *Biochim Biophys Acta* **1754**, 245–252 (2005).
24. Uehata, M. *et al.* Calcium sensitization of smooth muscle mediated by a Rho-associated protein kinase in hypertension. *Nature* **389**, 990–994 (1997).
25. Meyer, T. N. *et al.* Rho kinase acts at separate steps in ureteric bud and metanephric mesenchyme morphogenesis during kidney development. *Differentiation* **74**, 638–647 (2006).
26. Ewald, A. J., Brenot, A., Duong, M., Chan, B. S. & Werb, Z. Collective epithelial migration and cell rearrangements drive mammary branching morphogenesis. *Dev Cell* **14**, 570–581 (2008).
27. Hosen, N. *et al.* The Wilms' tumor gene WT1-GFP knock-in mouse reveals the dynamic regulation of WT1 expression in normal and leukemic hematopoiesis. *Leukemia* **21**, 1783–1791 (2007).
28. Armstrong, J. F., Pritchard-Jones, K., Bickmore, W. A., Hastie, N. D. & Bard, J. B. The expression of the Wilms' tumour gene, WT1, in the developing mammalian embryo. *Mech Dev* **40**, 85–97 (1993).
29. Davies, J. Control of calbindin-D28K expression in developing mouse kidney. *Dev Dyn* **199**, 45–51 (1994).
30. Grobstein, C. Morphogenetic interaction between embryonic mouse tissues separated by a membrane filter. *Nature* **172**, 869–870 (1953).
31. Grobstein, C. Inductive interactions in the development of the mouse metanephros. *Journal of Experimental Zoology* **130**, 319–340 (1955).
32. Srinivas, S. *et al.* Cre reporter strains produced by targeted insertion of EYFP and ECFP into the ROSA26 locus. *BMC Dev Biol* **1**, 4 (2001).
33. Bouchard, M., Souabni, A. & Busslinger, M. Tissue-specific expression of cre recombinase from the Pax8 locus. *Genesis* **38**, 105–109 (2004).
34. Plachov, D. *et al.* Pax8, a murine paired box gene expressed in the developing excretory system and thyroid gland. *Development* **110**, 643–651 (1990).
35. Sordella, R. *et al.* Modulation of CREB activity by the Rho GTPase regulates cell and organism size during mouse embryonic development. *Dev Cell* **2**, 553–565 (2002).
36. Riento, K. & Ridley, A. J. Rocks: multifunctional kinases in cell behaviour. *Nat Rev Mol Cell Biol* **4**, 446–456 (2003).
37. Georgas, K. *et al.* Analysis of early nephron patterning reveals a role for distal RV proliferation in fusion to the ureteric tip via a cap mesenchyme-derived connecting segment. *Dev Biol* **332**, 273–286 (2009).
38. Cho, E. A. *et al.* Differential expression and function of cadherin-6 during renal epithelium development. *Development* **125**, 803–812 (1998).
39. Essafi, A. *et al.* A wt1-controlled chromatin switching mechanism underpins tissue-specific wnt4 activation and repression. *Dev Cell* **21**, 559–574 (2011).
40. Cheng, H. T. *et al.* Notch2, but not Notch1, is required for proximal fate acquisition in the mammalian nephron. *Development* **134**, 801–811 (2007).
41. Sordella, R., Jiang, W., Chen, G. C., Curto, M. & Settleman, J. Modulation of Rho GTPase signaling regulates a switch between adipogenesis and myogenesis. *Cell* **113**, 147–158 (2003).
42. Reggiani, L., Raciti, D., Airik, R., Kispert, A. & Brandli, A. W. The prepattern transcription factor Irx3 directs nephron segment identity. *Genes Dev* **21**, 2358–2370 (2007).
43. Raciti, D. *et al.* Organization of the pronephric kidney revealed by large-scale gene expression mapping. *Genome Biol* **9**, R84 (2008).
44. Vivancos, V. *et al.* Wnt activity guides facial branchiomotor neuron migration, and involves the PCP pathway and JNK and ROCK kinases. *Neural Dev* **4**, 7 (2009).
45. Nishimura, T. & Takeichi, M. Shroom3-mediated recruitment of Rho kinases to the apical cell junctions regulates epithelial and neuroepithelial planar remodeling. *Development* **135**, 1493–1502 (2008).
46. Monier, B., Pelissier-Monier, A. & Sanson, B. Establishment and maintenance of compartmental boundaries: role of contractile actomyosin barriers. *Cell Mol Life Sci* **68**, 1897–1910 (2011).
47. Little, M. H. *et al.* A high-resolution anatomical ontology of the developing murine genitourinary tract. *Gene Expr Patterns* **7**, 680–699 (2007).


## Acknowledgements

We thank Paul Perry and Matthew Pearson for advice with time-lapse and confocal microscopy. We thank Rachel Berry and Anna Thornburn for providing the necessary animals. This work was supported by EuReGene, a Framework 6 program grant by the EU (05085) and the NC3Rs (G1000159).

## Author contributions

N.O.L. and J.A.D. designed the experiments and N.O.L. performed experiments. P.H. provided *Pax8*$^{Cre}$;*YFP*$^{lox\text{-}stop}$ and *Wt1*$^{+/GFP}$ models and assisted with manuscript preparations. N.O.L. and J.A.D. analysed experiments and wrote the manuscript.

## Additional information

**Supplementary information** accompanies this paper at http://www.nature.com/scientificreports

**Competing financial interests:** The authors declare no competing financial interests.

**How to cite this article:** Lindström, N.O., Hohenstein, P. & Davies, J.A. Nephrons require Rho-kinase for proximal-distal polarity development. *Sci. Rep.* **3**, 2692; DOI:10.1038/srep02692 (2013).